Ageing of Polymeric Surfaces Exhibiting Flow Marks—Effects on Surface Characteristics

G. Iannuzzi,[1] A. Nafari,[2] A. Boldizar,[1] M. Rigdahl[1]

[1]*Department of Materials and Manufacturing Technology, Chalmers University of Technology, Gothenburg, Sweden*
[2]*Nanofactory Instruments AB, 41288 Gothenburg, Sweden*

Received 1 July 2011; accepted 25 January 2012
DOI 10.1002/app.36893
Published online in Wiley Online Library (wileyonlinelibrary.com).

ABSTRACT: Surface defects associated with manufacturing processes can severely impair the appearance of polymeric products. These defects can be enhanced with ageing (time, UV-light, heat and weather conditions). In the present contribution, the interest is focused on the defects generated during injection molding of elastomer-modified polymers that are often used in the automotive sector to produce interior and exterior components. In particular, defects denoted as "flow marks" or "tiger stripes" were investigated. Two different grades of elastomer-modified polypropylene (PP)-containing mineral fillers were studied here before and after heat ageing for 9 weeks at a constant temperature of 95°C. Although injection moldings are one of the grades that did not exhibit any flow marks, moldings of other PP-grade showed such defects and they were enhanced after the ageing process. The properties and structure of the glossy and the dull bands (as well as the effect of the thermal ageing) have been assessed by several characteristics such as microhardness, nanohardness, crystallinity, and surface composition. An increase in surface hardness was noted after the ageing treatment as a consequence of increased crystallinity. Dull and glossy bands also exhibited different values of the nanohardness, glossy bands were harder, and the dull bands appeared to be less crystalline. The surface composition of glossy and dull regions was slightly different; the surface regions of the glossy areas contained higher amounts of filler particles. The effect of the ageing on the striped appearance is furthermore discussed in relation to possible depletion of the stabilizer system.
 J Appl Polym Sci 000: 000–000, 2012

Key words: poly(propylene); injection molding; ageing; degradation; surfaces

INTRODUCTION

A wide range of products are manufactured using polypropylene (PP)-based materials such as elastomer-modified PP-containing inorganic fillers. They are among the main materials for producing car bumpers, consoles, and other automotive components aiming at adequate or improved impact strength and other important mechanical properties. However, not only the functional properties are of importance in many applications, the appearance of polymeric components requires here increasing attention because the defects can lower the perceived quality of the final products. Needless to say, the visually perceived appearance is thus of great concern for most of the manufacturers of polymeric components.

Generally, automotive plastic components are manufactured by injection molding and, especially when the injection molding involves rather long flow lengths, defects such as "flow marks" or "tiger stripes" may appear.[1–5] Tiger stripes are usually characterized by alternating glossy and dull bands on the polymer surface, approximately perpendicular to the flow direction. Often, they are opposite in phase, that is, if one side of the molded part has a dull area, the corresponding area on the opposite side will be glossy.[4] The reasons for the formation of these effects are not entirely clear, but it has been proposed that flow instabilities during the mold filling, "slip-stick flow" or a combination of these can be the generating mechanisms.[1–3] It is, however, obvious that the regions corresponding to the dull and the glossy bands have experienced a difference in surface deformation during the mold filling. The rheological properties of the polymer melt may also play a role in this context; for example, a more pronounced elasticity of the melt has been reported to reduce the problem, cf. Refs. 6–8 and also the recovery behavior of the melt can be of importance.[9]

Automotive details of injection-molded PP-based materials are often used in exterior components and thus they are exposed to UV radiation, radiant heat, rain, humidity, etc. Therefore, a thorough understanding of the weather resistance and the degradation of the used polymeric materials is of great

Correspondence to: G. Iannuzzi (giovanna.iannuzzi@chalmers.se).
Contract grant sponsor: The Swedish Research Council and Chalmers University of Technology.

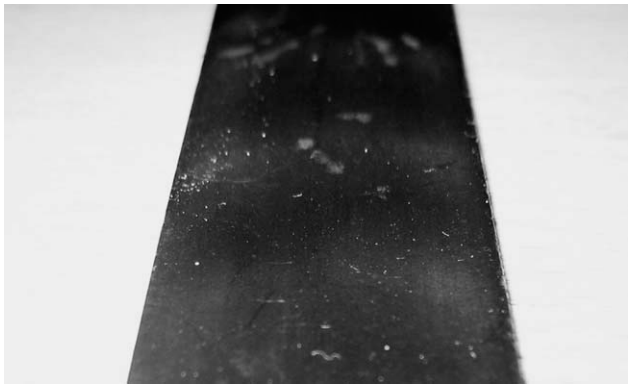

Figure 1 A test bar of modified PP exhibiting flow marks after exposure to Malaysian climate.

importance, not least in connection with the appearance of flow marks. In some cases, flow marks are initially almost invisible (right after molding) but they become more and more apparent after exposure to outdoor conditions.[10,11] More general, it is well known that polymeric materials can undergo degradation owing to sunlight and heat. This leads to loss of brightness, color changes, embrittlement, and formation of surface cracks.[12] An example of the visibility of the flow marks after exposure to the Malaysian climate is shown in Figure 1.

Several investigations have been carried out to determine the degradation behavior of (PP)-based materials, also with regard to the visibility of flow marks and similar defects.[10,11,13] Surfaces exposed to outdoor conditions generally show a rougher and less bright appearance compared to the original parts, but light-stabilizers and antioxidant agents can improve their weather resistance.[10,11] In some studies on elastomer-modified PP blends, it was clearly seen that ageing owing to UV light and heat exposure increased the visibility of flow marks changing the surface aspect of dull and glossy bands,[10,11] the first ones being affected more during the heat ageing as a result of their initially lower degree of crystallinity.[11] It was also reported that a number of micro-objects, that presumable contained rubber material, appeared on the surface of the dull stripes after the heat treatment.[11] In these types of materials, the rubber particles in the surface regions were more oriented in the glossy bands than in the dull ones (before any ageing treatment).[8,9] In their study on components aged during their service life, Iannuzzi et al.[4] noted that in the surface region of the dull bands the concentration of filler particles was lower than in the corresponding regions of the glossy bands.

In this study, emphasis has been given to the "flow marks" or "tiger stripes" formed on the surface of injection-molded elastomer-modified PP. Two different grades of this polymer containing mineral fillers were studied here before and after ageing for 9 weeks at a constant temperature of 95°C. Although one of the grades did not exhibit any flow marks, the other PP-grade showed such defects and they were enhanced after the ageing process. It was here of interest to clarify if the structure and the properties of the glossy and the dull bands differed in some important aspects and, if so, if the thermal ageing enhanced these differences. Improved knowledge on such differences can provide guidelines on how to reduce the detrimental effect of such defects on the surface appearance. Several characterization techniques were used for this purpose such as hardness measurements, estimation of the crystallinity, and assessment of the surface composition.

EXPERIMENTAL

Materials and preparation of specimens

Two grades of commercial elastomer-modified PP containing around 15 wt % talc as filler were used. They were denoted as B and C following the notation in the previous study in which these materials were employed.[7] Grade B had a density of 990 kg/m^3 and a melt flow index (230°C/2.16 kg) of 16 g/10 min. The corresponding data for Grade C were 1000 kg/m^3 and 18 g/10 min, respectively. Grade C has been reported to exhibit a lower melt viscosity than Grade B and also higher melt elasticity.[7] Moldings of Grade B exhibited flow marks, whereas those of Grade C did not. Test bars with the length 320 mm, the width 27 mm, and the thickness 2.5 mm were injection molded with the flow direction along the length of the specimens. Only one mold cavity was used for producing the specimens with one film gate. The mold temperature was set to 35°C, the melt temperature to 240°C, melt front speed 0.4 m/s, cooling time 13 s, total cycle time 34 s, and a holding pressure profile from 40 to 3 MPa (during the cycle). Some of the bars were thermally aged for 9 weeks at a constant temperature of 95°C in an oven with circulating air (no humidity control). A similar test bar of material B aged outdoors in Malaysia (typical climate temperature in the range of 22–33°C and relative humidity around 60%) was in some cases included as a comparison. The Malaysian samples are included only as a comparison or illustration. These specimens have also been subjected to UV degradation which makes a precise comparison with the thermally aged specimens less straight forward.

Characterization techniques

Several techniques were employed to characterize the structure and properties of the components. Measurements were carried out prior to and after heat ageing of both materials. Samples were taken

both from the front/cavity side and the back/ejector side of the injection-molded bars and from the different banded regions. Material C did not show any flow marks, neither before nor after ageing, whereas material B exhibited clear bands on both sides of the bars even before the ageing.

The surface structure of the test bars was examined by scanning electron microscopy, SEM, (Carl Zeiss DSM 940A digital scanning electron microscope, Germany). The instrument was equipped with a secondary electron detector. A Sputter Coater S150B, BOC Edwards, United Kingdom, was used for coating the surfaces of interest with a 5-nm thick gold layer before placing them in the microscope.

Stereo-pairs of SEM images, that is, two micrographs of the same specimen taken at two different viewing angles, can be combined to obtain a three-dimensional (3D) image (or model) of the analyzed area.[14] To combine the stereo-pairs, the software MeX 5.0 from Alicona Imaging GmbH was used. The 3D micrographs give the possibility to reproduce the surface topography and then calculate a measure of the surface roughness. In particular, the *root-mean-square roughness* S_q (eq. (1)) has been calculated to characterize the surface topography in the height direction over the analyzed area:

$$S_q = \sqrt{\frac{1}{A}\int_A z^2(x,y)\cdot dx\cdot dy} \tag{1}$$

where $z(x,y)$ is the surface height relative to the average surface area (profile) measured at the coordinates (x,y) of area A. The stereo-technique is described in detail elsewhere.[15,16]

Fourier transform infrared spectroscopy (FTIR) as well as electron spectroscopy for chemical analysis (ESCA) were used to evaluate the chemical composition of the surface of the test bars, in particular if any significant changes could be assessed owing to the heat aging or if there were any differences between the glossy and the dull bands. The FTIR-instrument used was a PerkinElmer System 2000 with a TGS detector performing ATR technique with a zinc-selenide crystal. The penetration depth is a few micrometers (<10 μm). The ESCA studies were performed with a PerkinElmer PHI 5500, USA, with a Al(K_α) X-ray source with energy of 1486.6 eV. The accelerating voltage was kept at 14 kV and the take-off angle was 45°.

Possible quantitative and qualitative differences in crystallinity between the specimens were estimated by means of X-ray diffraction (XRD). The instrument used was a Siemens D8 Advance Theta X-ray diffractometer with a CrK_α radiation source (wavelength, 0.22897 nm) equipped for low-angle XRD analysis.

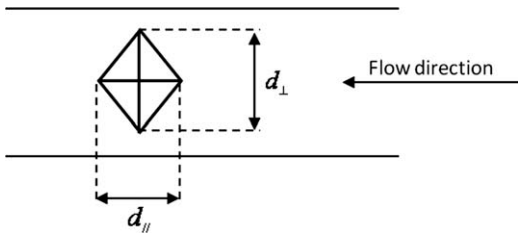

Figure 2 Schematic diagram of the impression from the Vickers intender and its orientation relative to the flow direction in the test bars.

For a similar purpose, differential scanning calorimetry (DSC) was also employed. The instrument used was a combined TG-DTA/DSC apparatus STA 449 F1 Jupiter from Netzsch-Gerätebau GmbH, Germany, equipped with a thermocouple Type K (Chromel-Alumel). From heating runs between 30 and 300°C in nitrogen atmosphere melting points and heats of fusion of the different samples were evaluated using a heating rate of 10°C/min. The heat of fusion provides a measure of the degree of crystallinity. The heat of fusion for a perfect crystal with a crystallinity of 100% of PP has been reported to be 198 J/g.[17] To analyze the thermal properties of the banded regions, thin slices, approximately 20–30 μm in thickness were cut (with a scalpel) from the surface of the bands. For each specimen, three to four runs were executed and the average values and standard deviations are reported.

To assess the differences in surface microhardness between the banded regions, a Shimadzu Micro Hardness Tester HMV-2000 was used. In short, a Vickers indenter, a pyramidal diamond indenter with a facing angle of 136°, penetrated the surface of the specimens with a known force leaving an impression of the diamond tip on the sample surface (Fig. 2).

Loads (weights) between 25 and 50 g were used and they were applied for 60 s. The hardness of the material is given in form of a Vickers microhardness number H_v (kg/mm^2):

$$H_v = \frac{F}{S} = \frac{2\sin\frac{\Theta}{2}}{d^2} = 1.854\frac{F}{d^2} \tag{2}$$

where F is the load (kgf), S the surface area of the indentation (mm^2), d the average diagonal of the indentation (mm), and Θ the angle of the pyramidal intender (°). In the measurements performed here, the depth of the indentations was between 20 and 40 μm. The indentations displayed a strong anisotropy owing to the orientation in the molded bars, cf. Ref. 18 The orientation in the flow direction leads to a higher elastic recovery in that direction and consequently to a smaller value of the diagonal $d_{||}$. Hence, the material would appear to be harder if

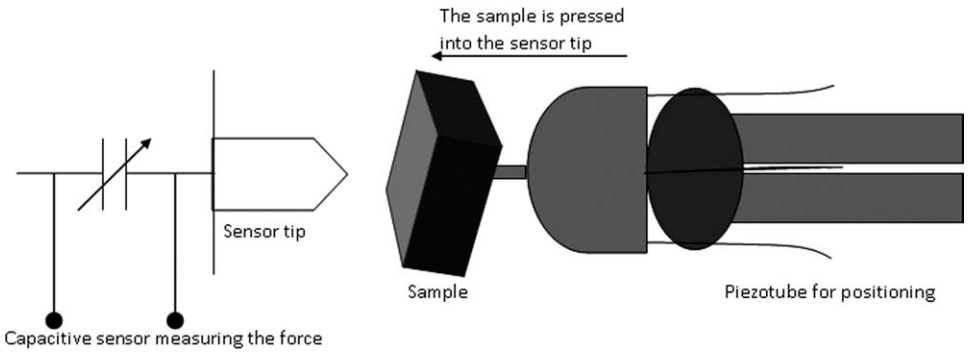

Figure 3 Sketch of the sensor and the sample. The sample is pressed into the sensor tip and the indentation force is measured with a capacitive sensor.

H_v is evaluated using $d_{\parallel}$ instead of $d_{\perp}$. An average value of the diagonals was used to determine the hardness value. Each hardness value was obtained as the average from 10 indentations.

Nanohardness measurements can be performed using an in situ transmission electron microscopy (TEM)-nanoindenter. Nanoindentations are used to investigate the mechanical properties of materials at the nanoscale[19] and in the present case they are expected to provide more information on the mechanical properties of the outermost surface layers than the microhardness measurements. To measure their surface nanohardness, the samples were pressed into a sharp diamond tip using a piezo-based positioning system, while collecting force–displacement data. The force was measured using a capacitive micromachined sensor on which a diamond tip was mounted. Figure 3 shows a sketch of the instrument used.

The TEM-nanoindenter system is presented in more detail in Refs. 20, 21 The nanohardness measurements included in this study were performed with an optical microscope, instead of a TEM, and a diamond tip with Berkovich geometry was used. The penetration depth into the surface was typically between 50 and 500 nm.

RESULTS AND DISCUSSION

Variations in gloss and surface roughness

As mentioned, the striped appearance of bars from material B was clearly visible and was enhanced by the thermal ageing, whereas no bands could be detected in case of the unaged or aged samples of material C. Although the variation in glossiness between the stripes (material B) was clearly visible, it was not possible to quantify it by means of a conventional glossmeter (obviously the naked eye is better sensor in this respect). The test bar exposed to the Malaysian climate exhibited, however, a gloss difference of about three gloss units, as measured with a standard glossmeter, which is to be considered as appreciable.

It was possible to assess some significant changes in the S_q-values between the glossy and the dull regions of samples of material B after the thermal ageing with the 3D SEM-technique. The S_q-values are summarized in Table I and were obtained using SEM stereo-pair images taken with a tilting angle of 5 and 10° at 200× magnification and applying data filtering with a cut-off length of 10 μm (to eliminate the influence of large-scale roughness/waviness). The dull regions were slightly more surface rough than the glossy ones as evident from Table I. The outdoor-aged Malaysian bar exhibited the same pattern of behavior. The surface roughness S_q of the unaged bars of material B did exhibit a similar pattern, that is, the glossy bands exhibit a lower S_q-value than the dull bands. The heat treatment as such produces, however, only a minor change of the surface roughness (typically an increase of the order of 0.01 μm or slightly higher).

This is in accordance to the results reported earlier in case of a component aged during its service life

TABLE I
Average Values of *Root-Mean-Square Roughness* S_q of Aged Specimens Obtained from Combining Stereo-Pair SEM Images Taken at a Relative Angle of 5°[a]

B—Front glossy 0.71 μm	B—Front dull 0.75 μm	B a—Back glossy 0.71 μm	B—Back dull 0.74 μm
B Malaysia—Glossy 0.80 μm	B Malaysia—Dull 0.84 μm		

[a] The standard deviation of the S_q values was <0.07 μm.

TABLE II
Average Values of Vickers MicroHardness (kg/mm^2) Determined Using Loads of 25 and 50 g[a]

	Material C unaged		Material C aged	
	Front	Back	Front	Back
H_v at 25 g	3.20	3.23	3.60	3.62
H_v at 50 g	3.28	3.23	3.60	3.67
	Material B unaged		Material B aged	
	Front dull	Front glossy	Front dull	Front glossy
H_v at 25 g	2.80	2.85	3.20	3.20
H_v at 50 g	2.93	3.04	3.31	3.39
	Material B unaged		Material B aged	
	Back dull	Back glossy	Back dull	Back glossy
H_v at 25 g	2.66	2.74	3.37	3.25
H_v at 50 g	2.82	2.89	3.44	3.55
			Material B Malaysian ageing	
			Front dull	Front glossy
Hv at 25 g			2.80	3.08
H_v at 50 g			3.38	3.42

[a] The standard deviation of the hardness values was <0.006 kg/mm^2.

for which clear differences in gloss and surface roughness could be assessed.[4] Higher values of the surface roughness of the dull regions after heat ageing at high temperatures have also been reported by Hirano et al.[11] The variation in surface roughness is also reflected in a corresponding variation in gloss (as discussed above) and color, for example the lightness.[22,23] Here, it can be added that no surface cracks or similar defects appeared owing to ageing of the test bars (as revealed by SEM).

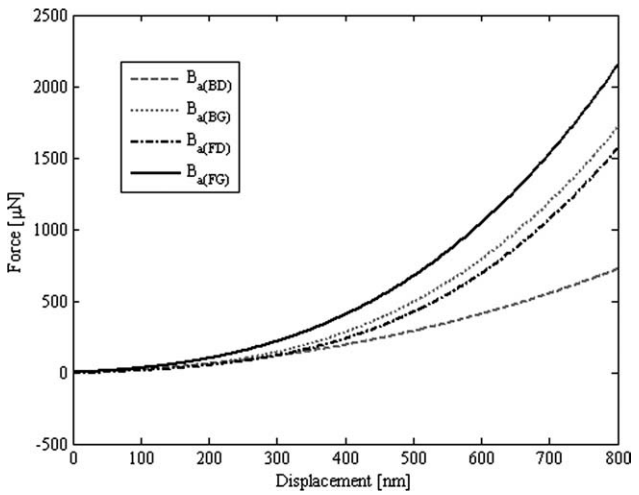

Figure 4 Force vs. displacement with the nanoindentor system for material B after ageing. The subscripts BD, BG, FD, and FG refer to back side dull, back side glossy, front side dull, and front side glossy, respectively.

Microhardness

The results of microhardness tests are summarized in Table II; the given hardness values correspond to loads of 25 and 50 g. It is clear that the microhardness increased owing to the heat ageing for both materials, which is also in agreement with the findings of Hirano et al.[11] A possible explanation is that the surface crystallinity increased when the samples were exposed to heat for a period of time. Bars of material C exhibited, in general, a higher microhardness than those of the other material which could be

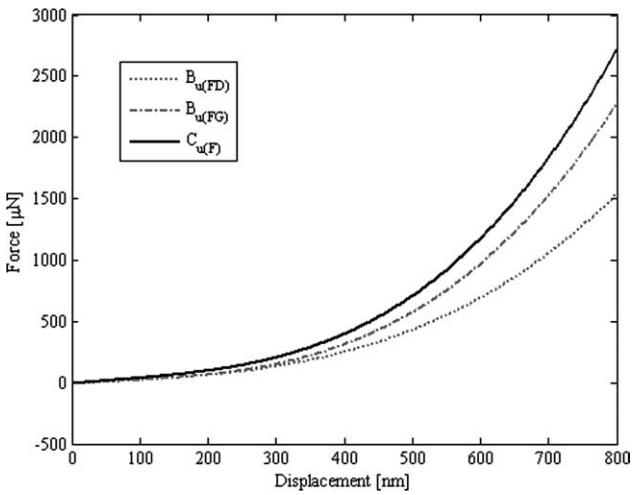

Figure 5 Same as Fig. 4, but comparing material B (front side) with C (front side) before heat ageing.

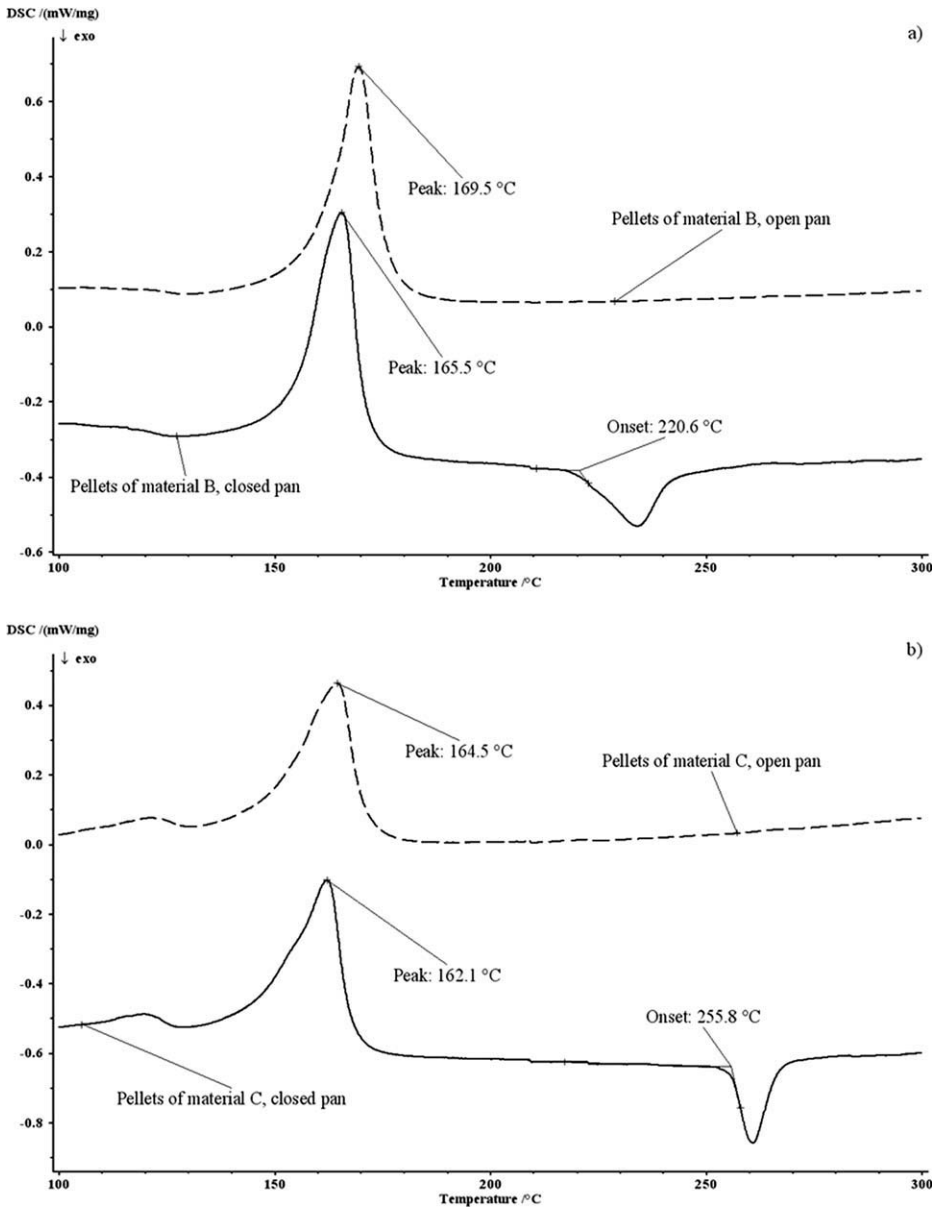

Figure 6 Examples of DSC endotherms for pellets of materials B (a) and C (b) obtained with and without holes in the pans.

associated with a higher crystallinity (cf. XRD-results) and/or a difference in filler content in the surface regions. It may be the fact that this is related to the propensity of the polymer to exhibit flow marks as there was a difference in the filler distribution in the surface regions between the bands, cf. Ref. 4 In case of material B, the dull bands were in general somewhat softer than the glossy ones. This was also noted for the test bar aged as it outdoors in Malaysia. Here, it should be pointed out that the intender penetrated the surface quite deeply and this may, to some extent, obscure any difference between the surface hardness of the stripes. SEM has actually revealed that the skin layer was thicker than the indentation depth but the difference was not great. These results are also consistent with the findings reported in Ref. 11, that is, the glossy bands exhibit a higher surface hardness than the dull regions. However, in some contrast, the present study did not reveal an increase in the hardness difference between the bands owing to the heat treatment.

Nanohardness

The nanohardness measurements were carried out on materials B and C before and after ageing for 9 weeks at 95°C. Samples of dull and glossy bands were taken from both the front side (denoted as F in Figs. 4 and 5) and the back side (denoted as B) of the injection-molded bars of material B. Also, in the case of material C, samples were taken from both sides of the test bars.

TABLE III
The melting points, the heats of fusion, the onset temperature of the exothermic peak and the corresponding peak temperature for the PP-based specimens[a]

	Melting endotherm		Exothermic peak	
Material	T_m, (°C)	ΔH_f (J/g)	Onset temp (°C)	Peak temp (°C)
B, pellet, open[b]	168 (0.6)	47.4 (2.6)	–	–
B, pellet, closed	166 (0.6)	50.7 (0.2)	224 (5.2)	236 (3.2)
B, unaged dull	165 (0.5)	51.6 (2.0)	209 (0.5)	218 (0.7)
B, unaged glossy	165 (0,9)	56.1 (0.1)	208 (2.1)	215 (0.6)
B, aged dull	165 (0.4)	50.9 (4.8)	179 (5.7)	200 (5.0)
B, aged glossy	165 (1.0)	62.5 (2.1)	194 (4.8)	208 (9.9)
C, pellet, open	164 (0.7)	41.3 (4.2)	–	–
C, pellet, closed	162 (0.2)	49.3 (0)	258 (4.0)	263 (2.8)
C, unaged	163 (0.2)	53.6 (2.9)	246 (6.0)	251 (6.6)
C, aged	163 (0.1)	55.3 (1.8)	236 (0.3)	241 (0.6)

[a] The average values are reported and the corresponding standard deviations are given within parenthesis.
[b] open refers to a pan with a hole, closed to one without any hole.

Looking first at material B, both for the front and for the back side of the molded bars, the glossy bands exhibited a higher value of the force needed to move the sensor a certain displacement as shown in Figure 4 in case of the aged test bars. This means that the glossy bands, on the front and back sides, had a higher surface hardness, which is in line with the microhardness results. The front side of the bars also exhibited a somewhat higher nanohardness than the back side.

Material C had a slightly higher nanohardness than material B (Fig. 5), which parallels the results from the microhardness measurements, cf. Table I. Materials B and C did not exhibit any significant changes in nanohardness after the ageing treatment, which is in some contrast to the microhardness results.

Thermal analysis of the surface regions

Figure 6 shows DSC endotherms of the pellets used for manufacturing the test bars. The measurements were performed as described previously under nitrogen flow. However, in one series of experiments, a hole was made in the DSC pan, in another no hole was made. When there was no hole in the pan, a second exothermic peak appeared at a temperature appreciably above the melting point of PP. With a hole in the pan, no such peak appeared. An interpretation of the observed behavior would be that the exothermic peak is associated with degradation, thermal oxidation, of the polymer, as it is possible that some oxygen was trapped in the closed pan. It is known that thermal oxidation of PP can take place at these temperatures, cf. Ref. 24 As evident from the graph, the onset temperature for the exothermic reaction is lower in case of material B compared to that of material C. This points a difference in the stabilizer system. Table III summarizes the thermal properties of the specimens analyzed here.

In the following when analyzing the thermal behavior of the surface portions of the banded regions, no holes were made in the DSC pans. Admittedly, the removal of the surface layers from the test bars is associated with some uncertainty, which means that the results should be regarded as indications rather than absolute values. In Table III, the melting point T_m, taken as the peak temperature of the endotherm, the heat of fusion ΔH_f, the onset temperature of the exothermic peak, as well as its peak temperature are listed.

From the measurements, it is clear that the ageing had no significant on the melting point of the polymer. Even when recognizing the experimental scatter, there was in most cases a clear trend toward an increased crystallinity (given by the change in ΔH_f) owing to the thermal ageing of the specimens in agreement with the observations made by Hirano et al.[11] This is also in accordance with the microhardness measurements and the results from X-ray diffraction (below). The measured heats of fusion also point out that the degree of crystallinity was higher in the surface regions of the glossy bands of material B than in the dull areas, both before and after the heat treatment.

The exothermic peak exhibited an interesting behavior which could be worth commenting. It is also exemplified in Figure 7 in case of material B. The injection molding of the test bars gave a shift of the peak toward lower temperatures compared to the result for the pellets. The ageing at an elevated temperature produced a further shift downward. This might indicate a consumption of the stabilizing system, antioxidants, during processing and ageing.

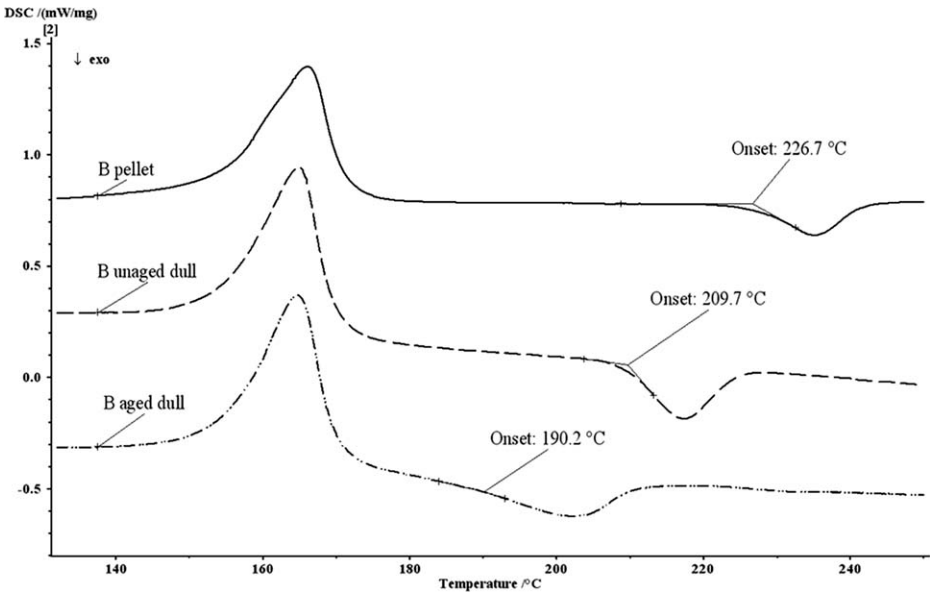

Figure 7 Examples of DSC endotherms for material B in the form of pellets, after injection molding (dull bands) and after ageing of the test bars (dull bands).

Material B appeared to be more sensitive than material C in this respect with a larger shift in temperature. It should be noted that the injection molding was performed with a melt temperature of 240°C and the onset of the exothermic reaction took place around 225°C (material B, pellets). The lowest onset temperature was observed for the dull bands of the aged material B being about 180°C, which would indicate that this region has become more susceptible to further degradation. Here, it may be noted that the rate of permeation of oxygen into the polymer can be lower if filler particles are present.[13,25] This may constitute an additional contribution to the more degraded appearance of the dull bands with less filler particles in the surface regions.[4]

Wide-angle XRD

When semi-crystalline polymers are analyzed with XRD, it is well known that the crystalline phase will give sharp diffraction peaks, whereas the amorphous component gives a very broad halo. The ratio between the corresponding integrated intensities can be used to estimate the degree of crystallinity in the material[26,27] based on a procedure outlined by Weidinger and Hermans.[28] Here, XRD has been used to identify qualitative differences in crystallinity between the two materials B and C as well as between-aged and unaged samples. The penetration depth of the X-rays can be estimated to be about 0.5 mm, cf. Ref.29, which means that differences in crystallinity between the dull and the glossy regions could be difficult to assess.

Figure 8 shows the XRD results obtained for both unaged and aged test bars of material B. The curves are shifted vertically to make the figure clearer. The diffraction peaks in the range of 20–32° (2θ) are associated with reflections from the (110), (040), (130), and (111) planes of PP. Diffraction peaks at lower and higher angles are likely to stem from the talc particles.[13] The PP-peaks became more pronounced (in relation to the amorphous halo) after the thermal ageing which indicates an increase in crystallinity, cf. also Ref. 11, which is in line with the increase in microhardness. The diffraction patterns for the dull and the glossy bands were very similar and no significant differences between the different bands could thus be ascertained, neither before nor after

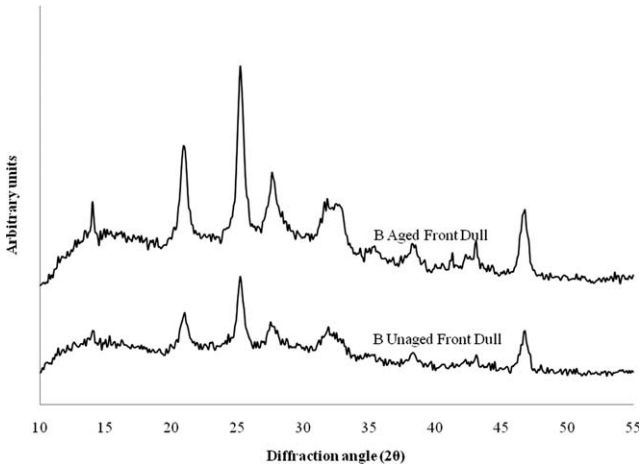

Figure 8 XRD profiles for unaged and aged test bars of material B.

the thermal ageing. This was not unexpected as mentioned earlier. Here, Hirano et al.[11] noted a lower crystallinity close to the surface of the dull bands compared to the glossy before the heat treatment, but after the ageing there was no difference in surface crystallinity.

In case of material C, the change in the diffractograms owing to the heat ageing was quite small. The diffraction peaks (associated with PP) for material C were, however, more pronounced compared to those for material B, pointing to a higher degree of crystallinity (data not shown) and material C also exhibited a higher microhardness than material B. Interestingly, the peaks stemming from the talc filler were significantly more intense in case of material B pointing to a difference in filler content between the materials, at least in the region given by the penetration depth of the X-rays. This may also have an effect on the degree of crystallinity of the surface regions. The influence of the filler particle distribution on the crystallization would, however, require a separate study and is beyond the scope of this article.

FTIR and ESCA

The glossy and the dull bands of aged test bars in material B were examined with FTIR. There were no appreciable differences between the spectra from the different regions, cf. Refs. 4,10 except in the wave number region 1000–1200 cm^{-1}. In this region, a rather broad absorbance peak was noted which presumably can be associated with the mineral filler, cf. Ref. 13 This peak was more pronounced for the glossy region, which is in line with the observation that the surface regions of these stripes contained more filler particles.[4]

In the ESCA studies of material B before and after ageing, the interest was focused on the C(1s)-peak which was separated into the components C1–C4. There were no significant differences between the spectra from the dull and the glossy regions. The only change that was noted was a small increase of the C2–C4 components (which are related to the carbon–oxygen bonds[30]) for material B owing to the thermal ageing. This could indicate some degradation.

FINAL REMARKS

Flow marks of the type considered here are most likely to be associated with flow instabilities, which can be induced by different mechanisms. It is known that the rheological properties of the melt, for example its elastic properties, can affect the generation of such defects. There also appears to be morphological differences between the glossy and the dull bands characterizing these flow defects such as a higher crystallinity in the surface regions of the glossy bands and a difference in filler content between the bands. Such differences were also evident from the surface hardness measurements, that is, the dull bands were, in general, softer than the glossy bands. A softer surface layer (with a somewhat higher roughness) is probably weaker and may be more susceptible to damage and contamination which would enhance the visibility of the flow marks during its service time (and ageing). Probably, these differences are confined to a rather thin surface layer, as they were not clearly revealed by all measuring methods.

In this context, it is tempting to speculate on the importance of the ageing stability of the material in relation to the visibility of the flow marks. The DSC measurements indicated that material B was more sensitive toward thermal oxidation and that there was a depletion of the stabilizer system during processing and ageing. Also, in case of material C there were indications of depletion, but it was less pronounced. Comparing the dull and the glossy bands of material B after ageing, it might be that there is less remaining active stabilizer in the dull bands, which probably can contribute to the visibility of the flow marks. The lower degree of crystallinity and filler content of the surface regions of these bands are likely to result in an increased sensitivity toward degradation (owing to an enhanced depletion/migration of the stabilizer) and an enhanced striped pattern with time. During the thermal treatment, the crystallinity increased which in principle can lead to the appearance of surface cracks, cf. Ref. 31 which can be expected to affect the stabilizer system and the appearance of the product.

Thus, the course of events during the mold filling coupled with the rheological behavior of the melt can result in a variation of the surface deformation of the component and an associated striped appearance. There may be a corresponding variation in morphology of the surface regions, leading to an alternating sensitivity toward surface degradation during ageing, that is, during the service life. Here, the choice of the stabilizer system can be of considerable importance as illustrated by the behavior of material B in the DSC measurements, at least in the case of PP-based materials of the kind considered here.

Plastal AS, Raufoss, Norway are thanked for injection molding of the test bars. The authors are also grateful to Livia Cerullo (Chalmers University of Technology, Sweden) for technical assistance.

References

1. Bulters, M.; Schepens, A. Proceedings of the 16th Annual Meeting Polymer Processing Society 2000, 144.

2. Grillet, A. M.; Bogaerds, A. C. B.; Peters, G. W. M.; Baaijens, F. P. T.; Bulters, M. J. Rheology 2002, 46, 651.
3. Hobbs, S. Y. Polym Eng Sci 1996, 36, 1489.
4. Iannuzzi, G.; Boldizar, A.; Rigdahl, M. Trans Nordic Rheol Soc 2009, 17, 157.
5. An, C.-C.; Chen, R.-H. J Mater Process Technol 2008, 201, 706.
6. Dharia, A. J. Inj Mold Technol 1999, 3, 67.
7. Iannuzzi, G.; Rigdahl, M. J. Appl Polym Sci 2010, 118, 604.
8. Hirano, K.; Suetsugu, Y.; Kanai, T. J Appl Polym Sci 2007, 104, 192.
9. Patham, B.; Papworth, P.; Jayaraman, K.; Shu, C.; Wolkowicz, M. D. J Appl Polym Sci 2005, 96, 423.
10. Hirano, K.; Tamura, S.; Kanai, T. J Appl Polym Sci 2007, 105, 2416.
11. Hirano, K.; Tamura, S.; Obata, Y.; Kanai, T. J Appl Polym Sci 2008, 108, 76.
12. Fechine, G. J. M.; Demarquette, N. R. Polym Eng Sci 2008, 48, 365.
13. Rabello, M. S.; White, J. R. Polym Compos 1996, 17, 691.
14. Janová, D. Czech J Phys 1994, 44, 255.
15. Ariño, R. Three-Dimensional SEM Characterization of the Topography of Polymeric Surfaces, Master Thesis, Chalmers University of Technology, 2008.
16. Ignell, S.; Ariño, R.; Iannuzzi, G.; Kleist, U.; Rigdahl, M. Polym Eng Sci 2010, 50, 1527.
17. González, V. A.; Alanís, M.; Guerrero, C.; Ortiz, U. J Polym Sci Part B: Polym Phys 2004, 42, 646.
18. Calleja, F. J. B.; Fakirov, S. Microhardness of Polymers; Cambridge University Press: Cambridge, UK, 2000.
19. Oliver, W. C.; Pharr, G. M. J Mater Res 1992, 7, 1564.
20. Nafari, A.; Angenete, J.; Svensson, K.; Sanz-Velasco, A.; Enoksson, P. J Micromech Microeng 2010, 20, 064017 (8pp).
21. Svensson, K.; Jompol, Y.; Olin, H.; Olsson, E. Rev Sci Instrum 2003, 74, 4945.
22. Judd, D.; Wyszecki, G. Color in Business, Science and Industry; John Wiley and Sons Inc.: New York, USA, 1975.
23. Ariño, I.; Kleist, U.; Rigdahl, M. Polym Eng Sci 2004, 44, 141.
24. Hoff, A.; Jacobsson, S. J. Appl Polym Sci 1984, 29, 465.
25. Barrer, R. M. Diffusion in Polymers; Academic Press: London, UK, 1968.
26. He, B. B. Two-Dimensional X-ray Diffraction; John Wiley & Sons: Hoboken, New Jersey, USA, 2009.
27. Rabello, M. S.; White, J. R. Polym Degrad Stab 1997, 56, 55.
28. Weidinger, A.; Hermans, P. H. Makromol Chem 1961, 50, 98.
29. Nishino, T.; Matsumoto, T.; Nakamae, K. Polym Eng Sci 2000, 40, 336.
30. Conners, T. E.; Banarjee, S. Surface Analysis of Paper; CRC Press Inc.: Baca Raton, Florida, USA, 1995.
31. Rabello, M. S.; White, J. R. Plast Rubber Comp Process Appl 1996, 25, 237.